REGULAR PAPER

Chaoqing Xu⬤ · Yi-Peng Liu · Zhechen Jiang · Guodao Sun · Li Jiang · Ronghua Liang

Visual interactive exploration and clustering of brain fiber tracts

Abstract Nuclear magnetic resonance images have been used for detecting the movement of water molecules in living organisms and moreover exploiting the neural fibers distribution, which is of great significance for the brain disease analysis. However, due to the visual clutter of dense fiber tracts, it is difficult for medical researchers to understand the water molecule diffusion in whole-brain scale and to find the meaningful substructure of neurological pathways. To address the challenges, we provide one fiber visualization workflow that combines fiber tracts selection and fiber clustering approaches with the advanced visualization technique. Local and global fiber selection methods are provided for users to extract fiber tracts with the higher strength of water molecule diffusivity and gain an overall perception of water molecule movement in whole-brain scale. To explore the substructure of brain fibers, we employ an anatomically meaningful similarity matrix combining with density peaks clustering algorithm and compare it with DBSCAN algorithm. The qualitative and quantitative experimental results show that the fiber visualization system helps to confirm the fiber distribution more accurately and efficiently.

1 Introduction

Diffusion-weighted imaging (DWI), diffusion tensor imaging (DTI), and high-angular-resolution diffusion imaging (HARDI) are advanced brain imaging techniques that allow noninvasive measurements for water diffusivity in biological tissues. By detecting the movement state of water molecules in the whole brain, researchers can analyze the brain activity in vivo and understand the physical structure of the whole brain, which is especially meaningful for the exploration of brain diseases. Fiber reconstruction and tracking techniques have been applied for generating the fiber tracts, which represent the neural tracts distribution in whole-brain scale. However, due to the visual clutter of dense fiber tracts, it is difficult for neuroscientists to find meaningful fiber tracts interactively and to explore the neurological pathways effectively (Fig. 1).

In order to explore brain fibers intuitively and efficiently, illumination techniques (Eichelbaum et al. 2013; Melek et al. 2006) are developed to render large numbers of dense fiber tracts. By applying the
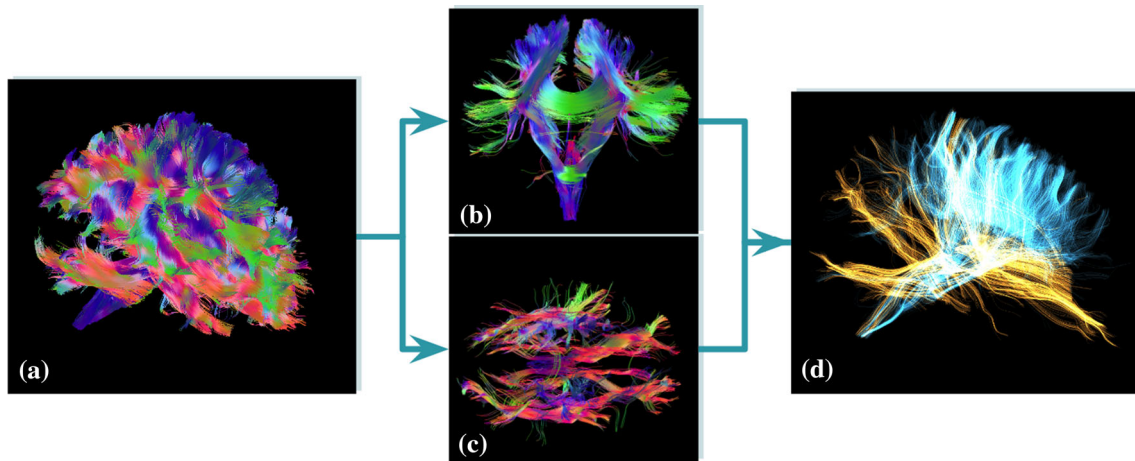
C. Xu · Z. Jiang
College of Information Engineering, Zhejiang University of Technology, Hangzhou, China

Y.-P. Liu (✉) · G. Sun · L. Jiang · R. Liang
College of Computer Science and Technology, Zhejiang University of Technology, Hangzhou, China
E-mail: liuyipeng@zjut.edu.cn

Fig. 1 Brain fiber selection and visual representations. **a** The visualization performance for the whole-brain fibers. **b** The fiber selection result with the global method ($C_l \in (-1.0, -0.5)$). **c** The fiber selection result with the global method ($C_l \in (0.8, 1.0)$). **d** Visual representation of the fibers with the recombination of the result in **b** and **c**

rendering technique, researchers are able to visualize complex spatial relations between dense fiber tracts. Geometric simplification methods (Enders et al. 2005; Weri et al. 2008) are presented for better understanding the overall white matter anatomy from the brain fiber tracts. Moreover, interactive systems are proposed for observing fiber connections in physical space, and users can extract the fiber tracts of interest by using geometric shape-based volumes (Sherbondy et al. 2005; Chamberland et al. 2014). In addition, researchers develop a variety of clustering methodologies for brain fiber analysis and intended to find the relationship between spatial clustering results and anatomical white matter structures in the human brain (O'Donnell et al. 2006; Sherbondy et al. 2005). Despite their successes, greater understanding of water molecule diffusion in whole-brain scale and the exploration of the meaningful physical structure is still challenging. Though multiple fiber rendering techniques and color mapping methods have been used for improving the visual quality and reducing overlaps between fiber tracts, it is still not sufficient for users to intuitively observe and interactively select fiber tracts based on water molecule diffusion intensity, which is of great value for brain research. While investigating the physical changes in the whole brain, it is difficult to identify which substructure of brain fibers is more discriminative for brain anatomy.

To help address these problems, we introduce one fiber visualization workflow that combines fiber tracts selection and fiber clustering approaches with the advanced visualization technique. Since fiber tracts are used to demonstrate the water molecules diffusion, meanwhile, they are presented as an overall trend of neurons. We hypothesize that the diffusion of water molecules, which appears as fiber tracts, contains important biological organization information and implies potential clues to the brain diseases. We provide two fiber selection methods based on local features and global features, respectively. The local selection method makes use of the direction of adjacent nodes, while the global selection method calculates the scatter matrix and the corresponding eigenvalues of each fiber. Additionally, in order to understand the substructure of brain fiber tracts in detail, we employ density peaks clustering (DPC) algorithm (Rodriguez and Laio 2014) combining with anatomically meaningful similarity matrix to study brain fiber pathways and extend the clustering algorithm to fit two types of brain fiber tracts. Density-based spatial clustering of applications with noise (DBSCAN) method (Ester et al. 1996) has been applied for the comparison with DPC. We conduct a qualitative and quantitative analysis of both clustering methods. Therefore, our contributions in this work are:

- We propose one brain fiber visualization workflow combining fiber selection and clustering for the exploration of water molecule diffusion in the whole brain as well as the substructures detection of brain fiber tracts.
- We develop two fiber selection methods for investigating water molecule diffusion state in whole-brain scale and selecting the fiber tracts of interest.

- We offer DPC algorithm combining with an anatomically meaningful similarity matrix to the study of brain fiber tracts. Both qualitative analysis and quantitative analysis are applied for the comparison with the DBSCAN algorithm.
- We present the interactive fiber visualization system for fiber extraction and recombination with the advanced rendering technique providing the overall perception of brain fibers and gaining a better understanding of their spatial relationship.

2 Related work

2.1 Fiber interaction methods

To explore and analyze brain fiber data efficiently and interactively, quite a number of studies have been provided by computer scientists, including geometry- and dimensionality reduction-based fiber interaction techniques.

Geometry-based fiber selection techniques have been commonly used for interactively selecting fiber tracts of interest. Sherbondy et al. (2005) present the dynamic query-based fiber selection method. By placing geometry shape-based volumes of interest (VIO), such as box-shaped or elliptical volumes, users can observe the fiber connection between the different brain regions interactively and efficiently. Similarly, Blaas et al. (2005) present the practical technique for interactively selecting fiber bundles in a full brain dataset using multiple convex objects. By the use of three selection boxes, users can independently select fiber bundles corresponding to specific brain function regions in real time. Chen et al. (2009) place multiple bounding boxes in fiber display window and code the fibers across these bounding boxes by different colors. Researchers can conveniently operate the fiber tracts by moving the bounding boxes and immediately visualize the fiber tracts in linked view. Cai et al. (2012) propose the fiber selection method for the dense DTI fiber tubes exploration. By the use of both boxes and spheres, multiple datasets selection, comparison, and visualization are allowed. Another interactive method uses the data features to detect brain fibers. Tax et al. (2015) selectively visualize fiber pathways based on the transparency of brain fiber bundles. Global and local fiber orientation has been used for color mapping, and researchers are able to visualize the brain fiber by changing the fiber opacity based on different fiber bundle directions and observation axis angles. Everts et al. (2015) propose the visualization technique for brain fiber tracts combining with fiber abstraction, selection, and interaction. It supports the selection of fiber tracts groups abstracted from the whole-brain datasets and provides insight into the structure of white matter through the visual abstraction and selection.

Dimension reduction-based fiber interactive techniques have been introduced for brain fibers research. By projecting the fiber tracts on three-dimensional space to a two-dimensional panel, researchers are able to gain more insight into brain structures and more effectively select fiber tracts of interest. Jianu et al. (2012) propose a 2D map-based fiber representation technique for solving the interaction complexity of brain fiber tracts in 3D physical space. It is faster and more accurate for users to select fiber bundles on the 2D fiber pathway representation than the 3D fiber bundles. Chen et al. (2009) introduce a fiber tract visualization system that combines dimension reduction, 2D space, and three-dimensional interactions. Users can select the fiber tracts on 2D space and immediately visualize DTI fiber tracts. Jianu et al. (2009) provide an interactive visualization workflow for investigating DTI fiber tracts with fiber abstraction, low-dimensional representations. Combining 3D modeling view with 2D representations, it can ease the navigation through complex fiber tracts. Jorge et al. (2012) present a multi-dimensional brain fiber data projection technology, by which fiber curvatures and spatial characteristics are projected to two-dimensional feature space. Researchers can simultaneously realize the interaction between feature space and three-dimensional physical space.

Though the success of the above-mentioned methodologies including geometry- and dimensionality reduction-based fiber selection from the complex brain bundles, the main consideration of which is the spatial structure of the fiber bundles, they are lack of the attention on the strength of water molecule diffusion in the brain space.

Positioning of our work Beyond the consideration of the physical relationship of brain fiber tracts, we provide two fiber selection methods for selecting the fiber tracts with higher strength of water molecule diffusion intensity, which has a great impact on the detection of brain anatomical structures.

2.2 3D streamline visualization

For the visualization of dense streamlines, simply rendering large number of lines always brings much visual clutter, which usually occludes important structures of the streamlines. It also brings difficulty to convey depth and spatial relationships. To solve those problems, computer scientists have came up with a variety of methodologies.

High-quality rendering techniques have been developed for solving the problem of occlusion and providing the higher spatial relationship of the dense streamlines. Everts et al. (2009) present the depth-dependent halos technique for illustrative visualization of 3D line datasets, such as DTI fiber tracts and fluid flow simulations. By using the depth-dependent halos, it is capable of producing high-quality black and white renderings and emphasizing line filtering and depth cueing. Researchers are able to visualize overall fiber structures within dense fiber tracts. LineAO (Eichelbaum et al. 2013) has been developed for solving the problem for complex spatial relations between dense bundles. With the use of global illumination, scientists are able to gain structural perception of line rendering in a very intuitive and natural way. Using the LineAO technique, scientists can visualize the structure fiber tracts intuitively; however, the occlusion is still remaining. Kuhn et al. (2013) present an efficient technique for the visualization of large amounts of trajectories. It allows to directly render 3D topological features and emphasize asymptotic topological features. Researchers are able to capture the intrinsic characteristics of different kinds of integration-based field lines.

In addition, studies for abstracting and emphasizing important structures and features from the dense streamlines have also been conducted. Günther et al. (2013) provide a globally optimal opacity-based line selection method for solving the occlusion problem of dense lines in the 3D field. By assigning varying opacities to the line segments, it supports a real-time navigation of the dense streamlines. The users can optionally define an important measure of the dense streamlines. Park et al. (2006) develop a geometry-based dense flow visualization method for directly visualizing the overall flow while providing structural insight into flow field data. Vector field visualization allows researchers to observe streamlines structures while gaining a dense overall representation. Everts et al. (2015) introduce a flexible illustrative line style model, which allows line parameters individually to depend on local attributes, for the visualization of streamline datasets. Moreover, a wide variety of lines visual representation abstracting and emphasizing line attributes can be obtained by changing the line style transfer function.

Positioning of our work Rather than developing a novel rendering technique for visualizing the whole structure of dense streamlines and extracting the important features of high-density line, we introduce those streamlines and important features, such as local orientation features and global orientation features, to the focus+context rendering. Even more, we provide an interactive visualization system supporting the overall perception of water molecule diffusion in the whole-brain scale and gaining a better understanding of their spatial relationship.

2.3 Trajectory clustering

Due to multiple forms among trajectories in human's brain, it is useful to apply clustering methods (Jin et al. 2014; Kim et al. 2005; Brun et al. 2003; Zheng et al. 2015; Liang et al. 2016) for categorizing those trajectories. Many advanced trajectory clustering techniques have been proposed for the brain fiber pathways exploration. Atlas-based clustering algorithms are commonly used, while movement clustering algorithms can also be extended to fiber trajectories.

Atlas-based clustering algorithms take brain anatomy information as a guide map for calculating similarities. To make the clustering result anatomical interpretable, researchers generally specify functional regions as cluster centers. Tun et al. (2014) design the framework composed of connectivity-based fiber representation, a fiber-based atlas, and an adaptive clustering algorithm, for automatically extracting brain fiber tracts groups that are similar to the fibers extracted by experts. Prasad et al. (2014) enable extracting, representing, and analyzing the geometry of white matter fiber tracts. By using the clustering algorithm, it makes population analysis of brain fiber tracts available. Atlas-guided clustering framework using hierarchical clustering analysis method has been presented to explore and analyze the large fiber tracts datasets (Ros et al. 2014). With the white matter atlas incorporated into the clustering algorithm, it is achievable to gain anatomically correct and reproducible fiber tracts.

Additionally, movement clustering algorithms have been applied for trajectory clustering and gained good results. Andrienko et al. (2018) provide an analytical workflow supporting for movement data analysis

by trajectory clustering, which is done using the similarity calculation method that ignores irrelevant elements, while the integrity of the trajectories is preserved. However, different distance functions settings have to be applied to multiple trails. Progressive clustering (Rinzivillo et al. 2008) explores heterogeneous properties of large numbers of trajectories by combining different types of distance functions. It reduces the computational complexity and makes the clustering result easier to interpret. Ferreira et al. (2012) introduce a model-based trajectory clustering technique by applying vector fields to the similarity calculation between trajectories. The similarity is calculated by trajectories together with their geometries, and the algorithm is able to capture the global pattern of noisy trajectories. Analogously, Wei et al. (2011) present a parallelization clustering algorithm for categorizing trajectories of large scientific data by leveraging the power of heterogeneous computers. The clustering method categorizing trajectories based on their space shapes works well with the large line data.

It is reproducible and understandable to extract fiber tracts close to anatomical regions while using atlas-based clustering; however, it increases the complexity for calculating the similarities of brain fibers. Oppositely, movement clustering methods consider much more about the physical structure of fiber tracts, which are lack of the consideration about anatomical information. It is imperative that both anatomical information and physical trajectory shapes are considered in the clustering algorithm and the calculation complexity is relatively acceptable.

Positioning of our work By giving more weight to those nodes close to the end of fiber tracts, the similarity matrix calculated is anatomically meaningful. Moreover, the DPC algorithm used for fiber tract clustering is affected by the physical spatial relationship between pairwise streamlines. Applying DPC with such a similarity matrix, we are able to acquire fiber clusters anatomical interpretable and time acceptable.

3 Methodology

To overcome the challenges on understanding the whole-brain fibers and efficiently finding the meaningful physical substructures, we provide the fiber visualization approach which integrates overall perception of the brain fiber pathways and the capability to explore the brain fibers details. Figure 2 shows the schematic diagram of our proposed visualization workflow. Due to the occlusion in original brain fibers, it is difficult for researchers to observe internal fibers. We provide local selection and global selection methods targeting at selecting fiber tracts with directional strength features. Researchers are able to extract the fiber pathways having strong water molecule diffusion and gain an overall perception of the water molecule diffusion in the whole brain. For detecting substructure of brain fibers, DBSCAN and DPC methods are applied. Qualitative analysis has been used for the comparison on the two clustering results and the corresponding anatomical structure in white matter.

In addition, we design the fiber interactive system with four basic steps. Firstly, we obtain two kinds of fiber orientations (local and global). Local fiber orientation is computed by the vector of neighbor points, and global fiber orientation is calculated from the scatter matrix for each fiber. Secondly, using the eigenvalues and eigenvectors from the previous step, we define two methods for selecting fibers from the whole brain and provide color coding methods. Also, we render the fibers by maximum Phong lighting (Mallo et al. 2005). Thirdly, iteratively over all the fibers, we calculate similarities between all pairs of fibers. Fourthly, we run a density peaks finding clustering algorithm (Rodriguez and Laio 2014) on the similarity matrix. Subsequently, we color these curves according to the clustering result. We will illustrate these steps with details in subsequent sections.
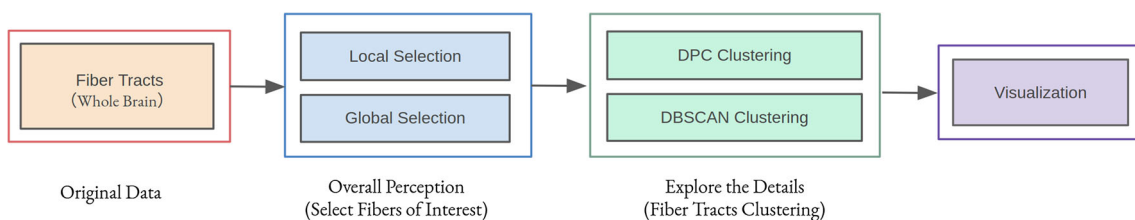
Fig. 2 Schematic diagram of the proposed visualization workflow

3.1 Fiber orientation

Though the orientation-dependent rendering technique has been used for fiber tract visualization (Tax et al. 2015), the local and global directions for color mapping bring a lot of occlusions, which brings interference to researchers when exploring the whole brain. Even more, such a color mapping method is not sufficient for researchers to observe the water molecule diffusion inside the brain. In this work, we extend the orientation-dependent technique for fiber tracts selection, rather than using it for color mapping. The orientation-dependent technique is mainly in two aspects: local orientation and global orientation. The local orientation is computed by adjacent two points, while the global orientation is computed by the scatter matrix of each fiber.

Local orientation We regard the streamline as a curve composed of points: $\gamma^1, \gamma^2, ...\gamma^i ..., \gamma^N$, where the point $\gamma^i = (x_i, y_i, z_i)$. The local orientation n_i at point γ^i, when i is not 1 and N, is figured out by the adjacent two points:

$$n_i = \frac{\gamma^{i+1} - \gamma^i}{\|\gamma^{i+1} - \gamma^i\|} = (\bar{x_i}, \bar{y_i}, \bar{z_i}) \tag{1}$$

where

$$\bar{x_i} = \frac{x_{i+1} - x_i}{\sqrt{(x_{i+1} - x_i)^2 + (y_{i+1} - y_i)^2 + (z_{i+1} - z_i)^2}},$$

$$\bar{y_i} = \frac{y_{i+1} - y_i}{\sqrt{(x_{i+1} - x_i)^2 + (y_{i+1} - y_i)^2 + (z_{i+1} - z_i)^2}},$$

$$\bar{z_i} = \frac{z_{i+1} - z_i}{\sqrt{(x_{i+1} - x_i)^2 + (y_{i+1} - y_i)^2 + (z_{i+1} - z_i)^2}}.$$

Global orientation Meanwhile, streamline orientation can also be regarded as the global one approximated by calculating the scatter matrix S.

$$S = \frac{1}{N} \sum_{i=1}^{N} n_i n_i^T \tag{2}$$

where n_i is the local orientation at the point γ_i and N is the amount of the streamline points. Then, we define a linear coefficient

$$C_l = \frac{\beta_1 - \beta_2}{\beta_1 + \beta_2 + \beta_3} \tag{3}$$

which ranges from -1 to 1, as an extra parameter for fiber selection where β_1, β_2, β_3, are the eigenvalues of scatter matrix S, and the eigenvalue β_1 is corresponding to the first eigenvector of S. Generally, the scatter matrix is not a symmetric matrix, so the eigenvalues are always complex numbers. In this case, we choose the real part of the eigenvalue instead of the eigenvalue. The eigenvalues can provide attribute information of the fiber data, especially when one eigenvalue is much larger than the others. In this occasion, a bipolar/bimodal distribution can be used to describe the fiber data very well, and we consider the eigenvectors of S as the streamline orientation. Then, these eigenvalues are used to color the streamlines.

3.2 Fibers selecting and color mapping

Once we get all the orientations of each fiber tract, orientation-based parameters indicating the intensity of water molecule diffusion strength can be extracted. The fiber tracts in the whole brain can be divided into different groups by adjusting parameter values. Users then can select brain fibers of different categories by using local and global direction parameters. In addition, for intuitively visualizing the water molecule diffusion state in the brain, simplified color mapping is introduced in this section.

Localselection We select fibers by counting the local orientation we get from the previous step. $\bar{x_i}, \bar{y_i}, \bar{z_i}$ can provide information on three directions and use colors to encode them. To ensure we have the correct range in RGB color space, we map n_i to RGB values

$$\begin{cases} R = & \bar{x}_i \times R_{max} \\ G = & \bar{y}_i \times G_{max} \\ B = & \bar{z}_i \times B_{max} \end{cases} \tag{4}$$

where $R_{max} = R_{max} = R_{max} = 255$. Then, we introduce three variables (U_{is}, U_{ap}, U_{lr}) to store the accumulations of local orientations, where U_{is} is used to store the accumulation inclined to the inferior–superior axis, U_{ap} and U_{lr} are used to store the accumulation inclined to the anterior–posterior and left–right axis, respectively. We use three indices ($\bar{x}_i$, $\bar{y}_i$, $\bar{z}_i$) and two parameters (w_1, w_2, where w_2 is much larger than w_1, here $w_1 = 0.3$, $w_2 = 0.95$) for fiber classification. It is well known that 30 degree is always regarded as the critical angle threshold for fiber tracking; in addition, 95% is considered as confidence intervals. Each fiber's local orientation n_i should be judged via the equation

$$\begin{cases} \|\bar{x}_i\| < w_1, \|\bar{y}_i\| < w_1, \|\bar{z}_i\| > w_2 & \rightarrow & U_{is} + 1 \\ \|\bar{x}_i\| < w_1, \|\bar{z}_i\| < w_1, \|\bar{y}_i\| > w_2 & \rightarrow & U_{ap} + 1 \\ \|\bar{y}_i\| < w_1, \|\bar{z}_i\| < w_1, \|\bar{x}_i\| > w_2 & \rightarrow & U_{lr} + 1 \end{cases} \tag{5}$$

The orientation accumulation of each fiber should be calculated. Each fiber tract belongs to one of the three categories, which is determined by calculating the maximum value of the three variables (U_{is}, U_{ap} and U_{lr}).

Moreover, each fiber has three indicators (deg_{is}, deg_{ap}, and deg_{lr}), which range from 0 to 100. The three indicators would be used to judge whether it should be rendered or not. They are calculated by the equation

$$\begin{cases} deg_{ap} = & \frac{U_{ap}}{U_{is}+U_{ap}+U_{lr}} \times 100\% \\ deg_{is} = & \frac{U_{ap}}{U_{is}+U_{ap}+U_{lr}} \times 100\% \\ deg_{lr} = & \frac{U_{ap}}{U_{is}+U_{ap}+U_{lr}} \times 100\% \end{cases} \tag{6}$$

Users first need to select the orientations of interest. Take the anterior–posterior orientation as an example. deg_{ap} of all the fibers will be calculated by the equation. Then, users need to specify a parameter deg for selecting the fibers. All the fibers with $deg_{ap} > deg$ would be selected and rendered. When deg is close to zero, we can see the fibers of the whole brain. Nevertheless, with the increasing deg, the brain fiber number is reducing.

Globalselection The eigenvectors of the scatter matrix, to the great extent, can describe the fiber orientations. According to equation (3), if β_1 is much larger than β_2 and β_3, C_l is a positive number close to 1. At this time, the first eigenvector expresses the dominant direction of the fiber. On the contrary, if β_2 is much larger than β_1, c_l is a negative number close to -1. In this case, the second eigenvector approximates the fiber orientation. Apart from these two cases, if the third eigenvector holds a dominant position, β_3 values greater than β_1 and β_2 and c_l approach 0. However, we find in most case, c_l is located in a relatively reasonable range from -0.65 to -0.1 or from 0.1 to 0.85.

On the basis of the result, we select fibers by giving a threshold interval about the coefficient c_l within the range from -1 to 1. When the threshold interval is an arbitrary segment of $(-1, 0]$, the corresponding fibers would be essentially in an inferior–superior direction. While the threshold interval is in the area of [0, 1), the relevant fibers would be mainly in the anterior–posterior direction. So we provide two alterable threshold intervals for fiber selecting, and the threshold intervals must be disjoint. Due to the feature that different signs represent different fiber orientations, in general, we will choose one threshold interval belonging to $c_l > 0$ and the other belonging to $c_l < 0$. In order to better display the structure information of the whole brain, we adjust the threshold range by experience and combine the fibers in different orientations. Then, two approaches are provided to color the fibers: The three eigenvectors can be used to describe the overall orientation of the fiber. For each fiber, we employ three eigenvalues to determine the RGB value and color the fibers by embedding them in the RGB color space:

$$\begin{cases} R = & Re(\beta_1) \times R_{max} \\ G = & Re(\beta_2) \times G_{max} \\ B = & Re(\beta_3) \times B_{max} \end{cases} \tag{7}$$
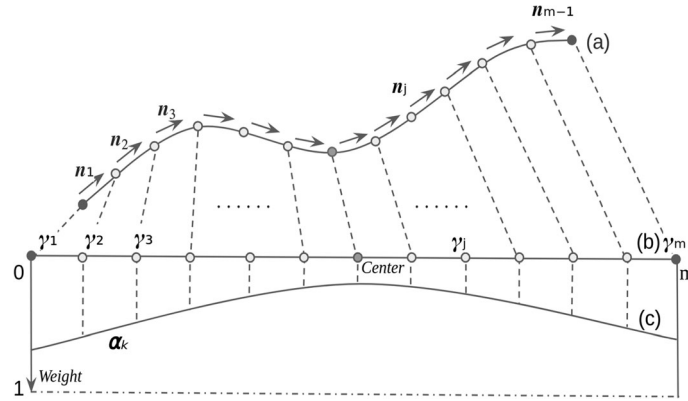
Fig. 3 Illustration of fiber tract and the weight of each node

where $R_{max} = R_{max} = R_{max} = 255$. Due to the eigenvalues (β_1, β_2, and β_3) of scatter matrix S would be complex numbers. $Re(\beta_1)$, $Re(\beta_2)$, and $Re(\beta_3)$ are presented as the real part of those eigenvalues. The real part can be used to indicate the directional characteristics of the fiber in three dimensions.

3.3 Similarities between fibers

Though a fiber from one functional region usually connects to several other functional regions, which makes the fiber tracts different shapes, we intend to identify the fibers connecting between different regions with high water molecule diffusion intensity. We hypothesize that the fiber tracts connecting two brain regions should have higher similarity, so we give more weight to the points closer to the ends of a fiber tract by the similarity calculation method (Demiralp and Laidlaw 2009).

Suppose that two fibers can be regard as $\gamma_i = \{\gamma_i^1, \gamma_i^2, \ldots, \gamma_i^m\}$ and $\gamma_j = \{\gamma_j^1, \gamma_j^2, \ldots, \gamma_j^n\}$ where m and n represent the amount of vertices, and we firstly compute the mean weighted distances between two fibers with the expression

$$d_{ij} = \frac{1}{m} \sum_{k=1}^{m} \alpha_i^k dist(\gamma_i^k, \gamma_j) \tag{8}$$

$$d_{ji} = \frac{1}{n} \sum_{k=1}^{n} \alpha_j^k dist(\gamma_j^k, \gamma_i) \tag{9}$$

where the function $dist(p, \gamma)$ returns the minimum Euclidean distance between the point p and the fiber γ. d_{ij} means the mean weighted distance from γ_i to γ_j, while d_{ji} is the opposite way. $\alpha_k = \frac{1}{Z} e^{|k-(m+1)/2|^2/\sigma^2}$ is used as a coordinating parameter with $Z = \sum_{k=1}^{m} e^{|k-(m+1)/2|^2/\sigma^2}$. We set the parameter $\sigma = \lambda L_\gamma$, where λ belongs to (0, 1] and L_γ is the length of the fiber. $\lambda = 0.5$ and $L_\gamma = 0.7m$ in practice. Figure 3 depicts a fiber tract and the weight of each node. Curve (a) is a fiber with the length m ($\gamma_1, \gamma_2, \ldots, \gamma_m$) and curve ($b$) shows the same fiber pathway after straightening. Curve (c) indicates the weight of each node in one fiber tract. Those nodes close to the end get higher weight and the center node get the minimum weight.

By providing the endpoints with higher weight, it should be able to make the similarity algorithm more sensitive to the endpoints, which are close to specific functional regions. The similarity matrix which combines the weight of each point and the Euclidean distance between a pair of trajectories can be used to classify the fiber tracts where the physical spatial and anatomical structure information is both considered.

3.4 Clustering

Brain fibers always contain different types of fiber pathways, which makes troubles for researchers to identify how many categories the fibers should be grouped into. Moreover, the number of brain fiber tracts is usually very huge bringing computation burden. Due to the complexity and density of brain fibers, the clustering algorithm entails clustering dense data with arbitrary shapes .

Both the DBSCAN and DPC can be used to cluster data with arbitrarily shape. However, the adjustment of DBSCAN algorithm is relatively complicated, compared with DPC algorithm. Moreover, the combinations of the two parameters in DBSCAN would have the greater impact on the final clustering effect. The main weakness of DPC is manual selection for the cluster center. However, the fibers of interest need to be judged in conjunction with the neuroscientists experience, so it is acceptable to use DPC.

In order to cluster the brain fibers, the distance matrix is generated by calculating the distance of fiber tracts pairwisely. For each fiber's data i, we compute two attributes: the local density ρ_i and the specified distance δ_i, which means the distance between i and j, where j is the nearest fiber with the local density larger than i. The formulas are as follows:

$$\rho_i = \sum_{j \neq i} \chi(d_{ij} - d_c) \tag{10}$$

$$\delta_i = min_{j:\rho_j > \rho_i}(d_{ij}), \tag{11}$$

where d_{ij} is the value stored in the distance matrix, d_c is the cut-off distance, $\chi(x)$ can be regarded as a piecewise function, when $x < 0$, $\chi(x) = 1$; otherwise, $\chi(x) = 0$. We take the fiber with the value of ρ_i and δ_i much larger than those of others as the cluster center. After finding the cluster center, we have to assign the remaining fibers to the nearest cluster where the density is higher.

When the data size is huge, the result is not easily influenced by d_c. The whole fiber number we use is 32038; nevertheless, after selecting through c_l, the selected fiber number will be hundreds to thousands. To further avoid this pitfall, we use Cheng (1995) to calculate ρ_i, and the formula is:

$$\rho_i = \sum_{j \neq i} \exp\left(-\left(\frac{d_{ij}}{d_c}\right)^2\right). \tag{12}$$

In this way, we can reduce the influence of d_c to the local density. According to the d_c processing ways, we divide the DPC method into two parts: DPC with the Gaussian kernel denoted as DPC(GK) or not as DPC(NGK).

4 Experimental results and discussion

In this section, the effects of our workflow on brain fiber visualization are discussed. Firstly, we will show the results of the local and global fiber selection methods. Second, our fiber visualization system will show that it contains the facilities of fiber division and fiber recombination. We also develop the focus+context visualization technique to better render the fibers and understand the fiber structure. Third, the clustering effect by DPC and DBSCAN and the algorithm evaluation will be displayed.

To measure the performance of the DBSCAN algorithm and the DPC algorithm, we use one PC with two Intel(R) Xeon E5-2670 processors, 8GB RAM, and NVIDIA Quadro 7000 graphics card, running at 2.60GHZ. Two clustering algorithms are both written in C++, while the visualization program is written by Qt and OpenGL. The development platform is Visual Studio 2010.
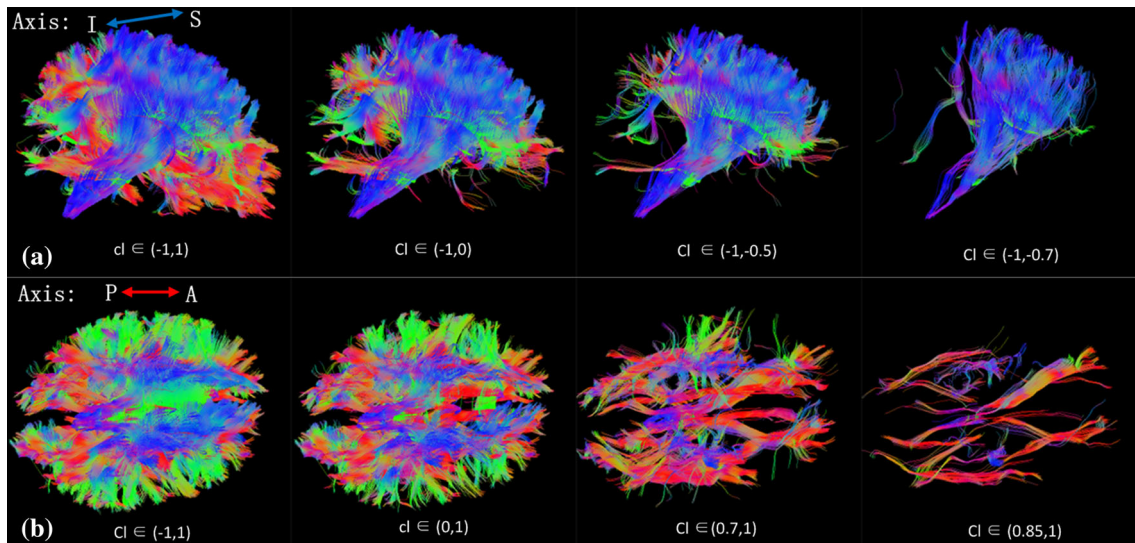
4.1 Fibers selection results

In this subsection, we will show how the orientation-based parameters influence the fiber selection result by gradually increasing or decreasing the parameter values. Then, we will have a qualitative comparison and get an overview of water molecule diffusion in the whole brain.

The local method Figure 4 shows some representative fiber selection results of different *deg* values along with different orientations. Figure 4a shows the fibers mostly in inferior–superior orientation (the blue fibers). In this row, *deg* increases from left to right. *deg* = 0 shows a conventional whole-brain fiber tractography rendering, where we cannot deeply observe inner fibers. With *deg* increasing, the fibers become more and more concentrated in the inferior–superior direction. When *deg* reaches 25, we can extract the main part of the fibers in the inferior–superior direction, though some fibers still contain the part of the red. Figure 4b shows the fibers mainly in the anterior–posterior orientation (the red fibers). As Fig. 4a, when *deg* comes to 0, the conventional whole-brain fiber cannot be directly detected. However, with *deg* reducing, the structure of the anterior–posterior direction fibers slowly emerges. When *deg* reaches 5, the fibers in the left–
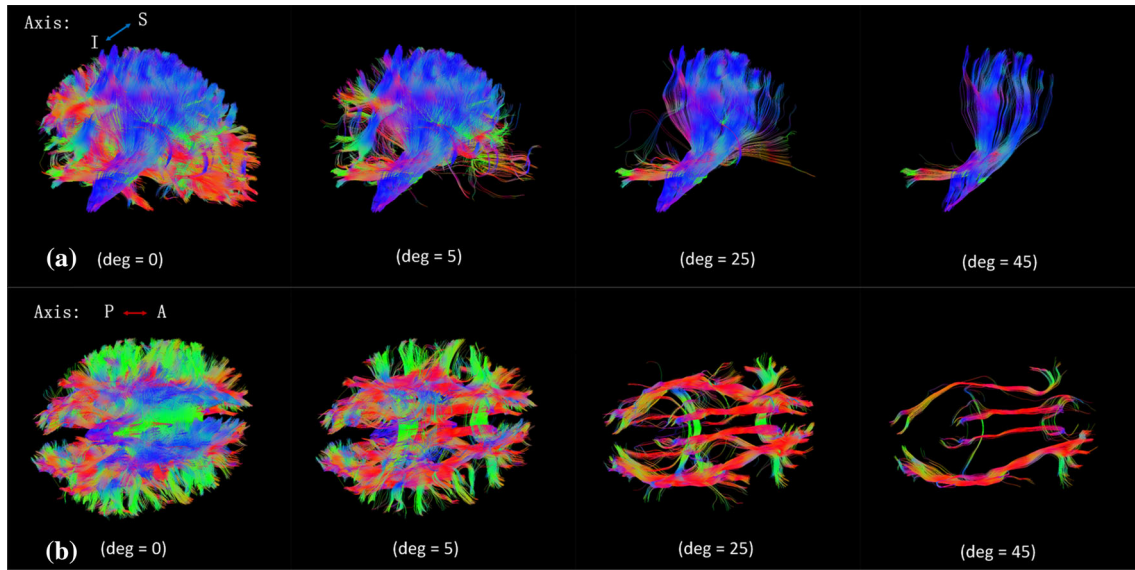
Fig. 4 Local method: Local selection results with different coefficient values, but fixed along different orientations. **a** The local selection results inclined to inferior–superior axis. **b** The local selection results inclined to the anterior–posterior axis

Fig. 5 Global method: global selection results with different threshold intervals, but fixed along different orientations. **a** The global selection results inclined to inferior–superior axis. **b** The global selection results inclined to the anterior–posterior axis

right direction (the green fibers) reduce obviously. As *deg* continues to reduce, the structure of the fibers in the anterior–posterior direction is completely revealed. As shown in Fig. 4b, when *deg* = 25, the blue fibers almost disappear; meanwhile, the green fibers greatly diminish. Even to the extent that the red fibers have been simplified when *deg* reaches 45, we can find the skeleton fibers in the anterior–posterior direction of the whole brain.

The global method Figure 5 shows the global selection method result in dealing with different threshold intervals along with inferior–superior and anterior–posterior orientations. Figure 5a shows the selection result with the linear coefficient $c_l < 0$; similarly, Fig. 5b shows the result with $c_l > 0$. In this view, the left column is the conventional whole-brain fiber visualization effect where the coefficient c_l belongs to (−1, 1). The second column $c_l \in (−1, 0)$ and $c_l \in (0, 1)$ divide the whole brain into two parts. From left to right, the threshold interval $c_l < 0$ comes to −1 and the threshold interval $c_l > 0$ comes to 1. When the c_l threshold interval reaches (−1, −0.5), the red fibers mostly disappear, while when the c_l threshold interval attains (0.7,

1), most of the blue fibers fade away. As the threshold intervals continuously shrink, the confidence related to the fiber and orientation consistency is getting higher and higher. When the c_l threshold interval drops to $(-1, -0.7)$, the main part of the blue fibers indicates that inferior–superior direction emerges, while when the c_l threshold interval rises to $(0.85, 1)$, the red fibers structure shows up.

Qualitative comparison As we can see in Figs. 4 and 5, both the local method and global method are capable of extracting the brain fibers structure. Nevertheless, the extracted results have different patterns. The blue fibers of the local method are less than those of the global method, and the structure of the local method is simpler. The blue fibers indicate the water molecule diffusion of inferior–superior direction, and the red fibers indicate the anterior–posterior direction. The reason for this phenomenon is that the structure extracted by the local method is related to the fiber length, whereas the global method only considers the direction of the whole fibers. When the number of nodes is smaller than *deg*, it will not be calculated. When it comes to the global method, it just only considers the general orientation of the fibers and has nothing to do with the fiber length, so the short fibers can also be sent to the cluster.

It seems that the local selection method is sensitive to the local orientation of the fiber and can be used to select fibers with very high curvature or very tortuous fibers. However, since the local selection method mainly considers the orientation information in three directions, it cannot judge the oblique fiber well, and the oblique diffusion of water molecules cannot be well captured. Oppositely, the global selection method is very sensitive to the overall orientation of the fiber, and it can be used to select fibers with similar directions at a global angle. It has the advantage of capturing the oblique fiber, which is the drawback of the local selection method. But the disadvantage of global selection method is that the local orientation of the fiber cannot be well judged. Once the curvature of the fiber is too large, it may not be well selected. Overall, these two fiber selection methods are complementary and users can select the vast majority of the fibers.

Figure 8 shows the fiber tracts extracted using the two fiber selection methods and the cooresponding anatomical structures. Figure 8a shows the fiber tracts extracted using local selection method with the parameter $deg = 25$, and Fig. 8b shows the fiber tracts extracted using global selection method with the parameter $c_l \in (-1, -0.5)$. Figure 8c presents the cortical–spinal tracts (Cort.Spinal.Tr) connecting between two brain regions extracted by the anatomical structure. By visually comparing these three figures, we learned that both selection methods can be used to extract fibers anatomically meaningful. Combining with Figs. 4 and 5, we can clearly see that fibers gradually change with parameters adjustment operation.

4.2 The fibers visualization system

We present an interactive system for fiber extraction and recombination with focus+context visualization technique providing an overall perception of brain fibers and gaining a better understanding of their spatial relationship.

System introduction The interactive system interface is shown in Fig. 6, which consists of three main parts: two interactive windows of c_l on the left and a main display window on the right. The two interactive
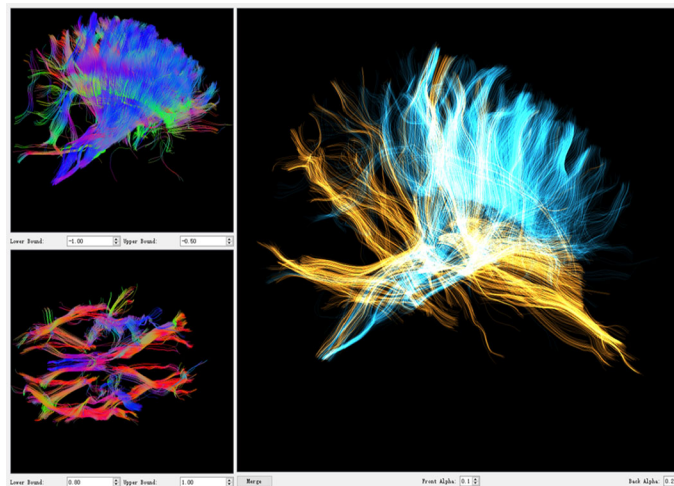
Fig. 6 An interactive fiber visualization system for fiber selection and recombination
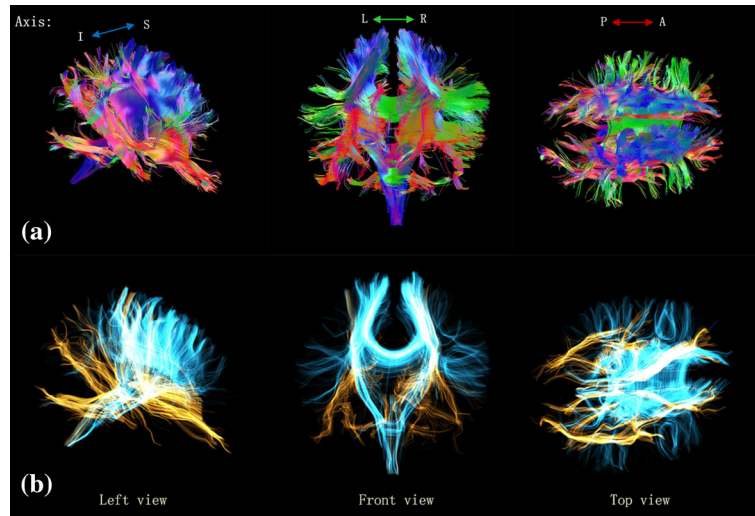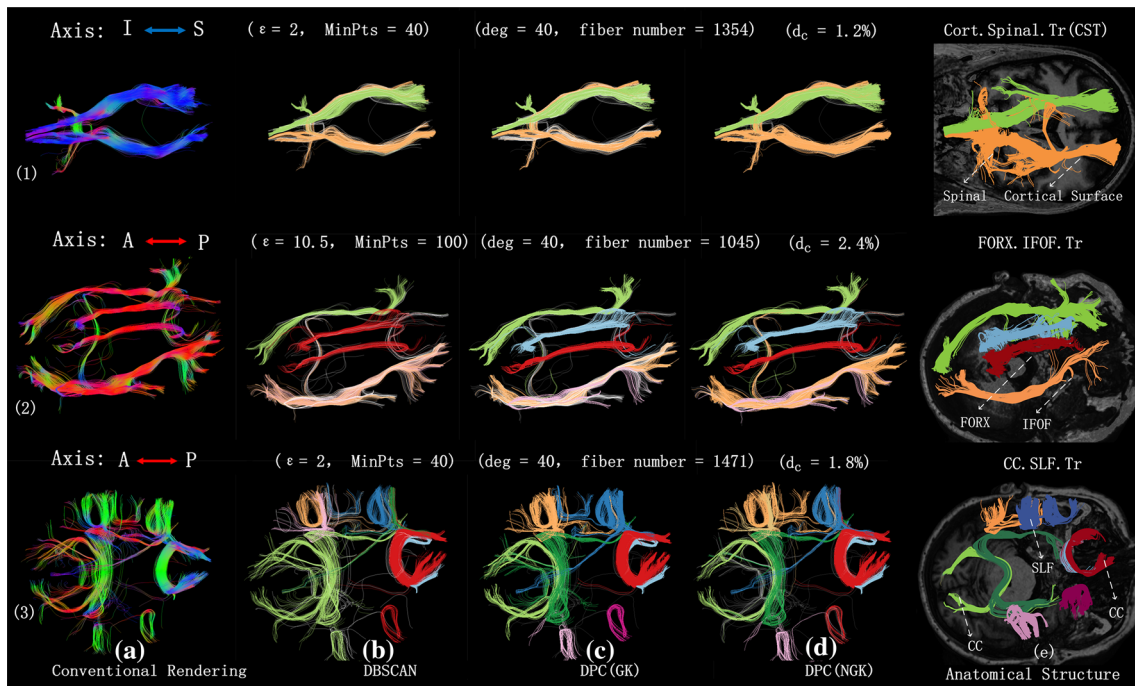
Fig. 7 The comparison of the conventional fiber rendering and focus + context visualization in three views
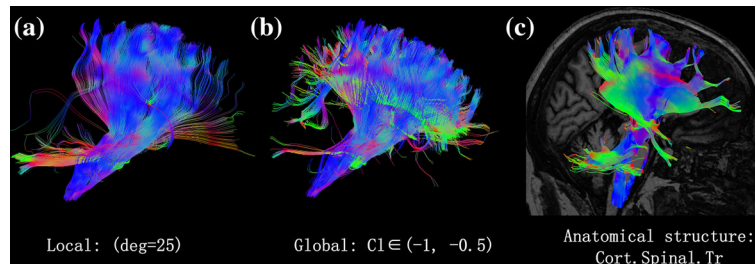
Fig. 8 A qualitative comparison of the fiber tracts extracted using local selection method, global selection method, and anatomical structures

windows are used to display the fibers in real time by clicking the c_l selection components lying down on the bottom of each window. The values on the left must be smaller than the right side. Usually, we choose the threshold interval across over 0. By this way, we can obtain two groups of fibers with different orientations in the display windows. After getting the two part of the fibers selected from the whole brain, we further combine them together on the right window encoded by the conventional RGB color space. In this case, brain fibers still have many occlusions so that we cannot find the relations of brain fiber structure and we cannot investigate how water molecule diffuses in the whole brain. To solve this problem, we introduce an illustrative focus+context visualization technique to render the fibers and change the color and opacity. We can, respectively, preset the colors of the two selected fibers, and on the bottom of the main window, we provide two opacity adjustment buttons.

Rendering results After fiber selection, we combine the two parts of the fibers together and render them, respectively. The rendering results are shown in Fig. 7. From left to right, the figures are shown as left view, front view, and top view, respectively. Figure 7a indicates the original rendering that use the RGB space, and Fig. 7b shows the fibers focus+context visualization results. We can easily find that the inner fibers of the original rendering cannot be seen. Owing to the occlusion of fibers in all orientations, viewers cannot understand the spatial relations inside the brain, but a glance on the surface. It is not sufficient to just simply observe and understand the structure of fiber tracts. Researchers are not able to gain any insight into water molecule diffusion inside the brain, while through the focus+context visualization technology, the selection fibers are colored in golden and light blue. The golden fibers are those fibers in the anterior–posterior direction, while most light blue fibers are in the inferior–superior direction. The two types of fibers are well bedded, and users can clearly observe the golden fibers in the top view. And in the left view and front view, we can find the fibers overlapped intuitively, because the crossing fibers are rendered with white color. Also, we are able to separately show the two groups fibers. Above all, by using the focus+context visualization technology, we can better detect the fiber structure and understand the spatial location of the fibers with

Fig. 9 A qualitative comparison of the conventional rendering of the extracted fiber tracts, cluster results of those fibers, and corresponding anatomical structures

respect to the brain organization structure. Researchers can immediately have an intuitive impression of water molecule diffusion state in the whole brain (Fig. 8).

4.3 Clustering results and performance evaluation

Besides selecting brain fiber tracts and gaining more insight into the water molecule diffusion in the brain, we provide clustering methodologies for detecting the substructures of brain fibers. With higher weight laid on those nodes close to the fiber endpoints, our clustering results can be anatomically interpretable.

DBSCAN and DPC have been employed in our paper. In addition, We classify DPC into DPC(GK) and DPC(NGK) based on the d_c processing way, which is a parameter influenced by data size. Those fiber tracts selected by our previous steps are used for clustering, as shown in each row of Fig. 9. The first row of Fig. 9 reveals the fibers in the inferior–superior direction (blue fibers), the second row reveals the anterior–posterior fibers (red fibers), and the last row reveals the left–right fibers (green fibers). Each column indicates different types of fiber tracts.

Figure 9a shows the original fiber tracts extracted from the previous step with conventional rendering. The second column to the fourth column (Fig. 9b–d) are the clustering results of DBSCAN, DPC(GK), and DPC(NGK), respectively. Figure 9e shows the fibers extracted by FreeSurfer (2012) using brain connectome, which shows the inner connections of brain functional regions. From Fig. 1, we can find that the fibers that extracted by our fiber selection methods seem anatomically meaningful. In order to explain it accurately, we specify the particular figure through different rows and columns labels. For example, Fig. 9b-3 refers to the figure in the second column and the third row. Figure 9e-1 shows the fiber tracts of substantial nigra region (a functional region in mid-brain) that connects cortical surface and spinal. Figure 9e-2 shows the inferior fronto-occipital fasciculus (IFOF) along fornix, which is a C-shaped fibers bundle in the brain. Figure 9e-3 is the part of superior longitudinal fasciculus fibers in corpus callosum (CC) region connecting among different lobes.

When investigating the brain fibers and the clustering results, we provide a qualitative comparison with fibers extracted through anatomical structures. It is obvious that fibers extracted by our fiber selection methods seem very similar to those selected by anatomical structures. Moreover, it is clear that the DPC results of the fiber tracts, as shown in Fig. 9c, d, have higher similarity with those fiber tracts in Fig. 9e than DBSCAN in Fig. 9b. Through such a qualitative comparison, we can confirm that the current clustering

Table 1 Comparison of DBSCAN and DPC

Fiber data (#Fiber)	DBSCAN			DPC(GK)	DPC(NGK)	
	ϵ	*MinPts*	time/ms	time/ms	d_c/%	time/ms
Blue fibers (1354)	2	40	153	229	1.2	102
Red fibers (1045)	10.5	100	94	124	2.4	61
Green fibers (1471)	2	40	256	253	1.8	118

algorithms can be used for exploring the substructure of brain fiber tracts, especially those inner connection fibers between different brain regions.

For the comparison of these clustering algorithms, we appropriately describe the clustering parameters of each clustering method. As shown in Fig. 9b, *e* and *MinPts* are two adjustable parameters of DBSCAN. *e* means the radius, while *MinPts* means the minimum number of points required to form a dense region. We regulate different parameter values for each fiber's data. They will have a great influence on the clustering result. d_c is the only parameter of DPC(NGK). We set $d_c = \frac{value}{max_{d_{ij}}} \times 100\%$. When finished clustering the fibers, we use corresponding colors to render the cluster results. The white fibers in the graphs do not belong to any cluster, so we regarded them as noise.

We can find that it is effective to separate fibers using DPC(GK), as shown in Fig. 9c, and fibers are clearly separated by different colors. In contrast, DPC(NGK) results of blue fibers and red fibers have less noise. However, DPC(NGK) clustering result in Fig. 9d-3 has more noise than the result in Fig. 9c-3. Even to the extent that the red cluster contains two groups of fibers which obviously should be divided into two categories. Compared with DPC results, DBSCAN results are not satisfactory in most case. In Fig. 9b-2, two longer fibers are regarded as one cluster. Meanwhile, we can find a similar phenomenon in the bottom of Fig. 9b-3. Obviously, the two categories (light green and red) should be divided into more categories as the DPC result.

From the clustering results above, we can confirm that the DPC algorithm has advantages in getting more discriminative substructures of brain fiber tracts, especially those inner connection fibers between different brain regions than the DBSCAN does. Both of the two DPC methods are able to get anatomically reasonable fiber tracts. Between the two DPC methods, DPC(NGK) allows the users to tune the parameter with less noise, while DPC(GK) can provide a more stable performance without adjusting parameters. Table 1 presents the computational cost of the DBSCAN algorithm, the DPC(GK) algorithm, and the DPC(NGK) algorithm. We see that the efficiency of DBSCAN outperforms that of DPC(GK). DPC(NGK) further improves the efficiency of DBSCAN. The larger the fiber tracts size, the advantage of the DPC(NGK) technique is more apparent.

5 Conclusion and future work

In this work, we present one visualization workflow that combines fiber tracts selection methods and fiber clustering approaches for investigating the overall water molecule diffusion in human brain and the understanding substructures of brain fiber pathways. Users can extract fiber tracts based on the intensity of water molecule diffusivity and gain overall perception through the focus+context fiber visualization system. Moreover, DPC and DBSCAN methods have also been applied for exploring the substructure of the brain fibers of interest. Through qualitative and quantitative analysis on the clustering results, we learned that the DPC method gains more advantages over the DBSCAN method for detecting microstructures in brain fiber tracts with various shapes.

However, our study are not without limitations: (1) The current local fiber selection methods are based on the horizontal and vertical orientations, and it is not sufficient to extract oblique and multiview twisted fiber tracts. In addition, quantitative analysis of the two fiber selection methods is needed. (2) The current clustering methods are calculated by Euclidean distance, which inevitably brings complexities.

In the future work, we desire to analyze the relevance between the brain fiber distribution and the specific nervous system disease for clinical diagnosis.

References

Andrienko G, Andrienko N, Fuchs G, Garcia JMC (2018) Clustering trajectories by relevant parts for air traffic analysis. IEEE Trans Visual Comput Gr 24(1):34–44. https://doi.org/10.1109/TVCG.2017.2744322

Blaas J, Botha CP, Peters B, Vos FM, Post FH (2005) Fast and reproducible fiber bundle selection in dti visualization. IEEE Visual 2005:59–64. https://doi.org/10.1109/VISUAL.2005.1532778

Brun A, Park H-J, Knutsson H, Westin C-F (2003) Coloring of dt-mri fiber traces using Laplacian eigenmaps. In: Moreno-Díaz R, Pichler F (eds) Computer aided systems theory—EUROCAST 2003. Springer, Berlin, pp 518–529

Cai H, Chen J, Auchus AP, Correia S, Laidlaw DH (2012) Inshape: in-situ shape-based interactive multiple-view exploration of diffusion mri visualizations. In: Bebis G, Boyle R, Parvin B, Koracin D, Fowlkes C, Wang S, Choi M-H, Mantler S, Schulze J, Acevedo D, Mueller K, Papka M (eds) Advances in visual computing. Springer, Berlin, pp 706–715

Chamberland M, Whittingstall K, Fortin D, Mathieu D, Descoteaux M (2014) Real-time multi-peak tractography for instantaneous connectivity display. Front Neuroinf 8:59. https://doi.org/10.3389/fninf.2014.00059

Chen W, Ding Z, Zhang S, MacKay-Brandt A, Correia S, Qu H, Crow JA, Tate DF, Yan Z, Peng Q (2009) A novel interface for interactive exploration of DTI fibers. IEEE Trans Visual Comput Gr 15(6):1433–1440. https://doi.org/10.1109/TVCG.2009.112

Cheng Y (1995) Mean shift, mode seeking, and clustering. IEEE Trans Pattern Anal Mach Intell 17(8):790–799. https://doi.org/10.1109/34.400568

Demiralp C, Laidlaw DH (2009) Similarity coloring of DTI fiber tracts. In: Proceedings of DMFC Workshop at MICCAI

Eichelbaum S, Hlawitschka M, Scheuermann G (2013) LineAO—improved three-dimensional line rendering. IEEE Trans Visual Comput Gr 19(3):433–445. https://doi.org/10.1109/TVCG.2012.142

Enders F, Sauber N, Merhof D, Hastreiter P, Nimsky C, Stamminger M (2005) Visualization of white matter tracts with wrapped streamlines. IEEE Visual 2005:51–58. https://doi.org/10.1109/VISUAL.2005.1532777

Ester M, Kriegel H-P, Sander J, Xu X (1996) A density-based algorithm for discovering clusters a density-based algorithm for discovering clusters in large spatial databases with noise. In: Proceedings of the 2nd international conference on knowledge discovery and data mining, KDD'96. AAAI Press, pp 226–231

Everts MH, Begue E, Bekker H, Roerdink JBTM, Isenberg T (2015) Exploration of the brain's white matter structure through visual abstraction and multi-scale local fiber tract contraction. IEEE Trans Visual Comput Gr 21(7):808–821. https://doi.org/10.1109/TVCG.2015.2403323

Everts MH, Bekker H, Roerdink JBTM, Isenberg T (2009) Depth-dependent halos: illustrative rendering of dense line data. IEEE Trans Visual Comput Gr 15(6):1299–1306. https://doi.org/10.1109/TVCG.2009.138

Everts MH, Bekker H, Roerdink JBTM, Isenberg T (2015) Interactive illustrative line styles and line style transfer functions for flow visualization

Ferreira N, Klosowski JT, Scheidegger C, Silva C (2012) Vector field k-means: Clustering trajectories by fitting multiple vector fields

Fischl B (2012) Freesurfer. NeuroImage 62(2):774–781. https://doi.org/10.1016/j.neuroimage.2012.01.021 20 YEARS OF fMRI

Günther T, Rössl C, Theisel H (2013) Opacity optimization for 3d line fields. ACM Trans Gr 32(4):120:1–120:8. https://doi.org/10.1145/2461912.2461930

Jianu R, Demiralp C, Laidlaw D (2009) Exploring 3d DTI fiber tracts with linked 2d representations. IEEE Trans Visual Comput Gr 15(6):1449–1456. https://doi.org/10.1109/TVCG.2009.141

Jianu R, Demiralp C, Laidlaw DH (2012) Exploring brain connectivity with two-dimensional neural maps. IEEE Trans Visual Comput Gr 18(6):978–987. https://doi.org/10.1109/TVCG.2011.82

Jin Y, Shi Y, Zhan L, Gutman B, de Zubicaray G, McMahon K, Wright M, Toga A, Thompson P (2014) Automatic clustering of white matter fibers in brain diffusion MRI with an application to genetics. NeuroImage 100:75–90. https://doi.org/10.1016/j.neuroimage.2014.04.048

Jorge P, Eler DM, Paulovich FV, Minghim R (2012) Employing 2d projections for fast visual exploration of large fiber tracking data. Comput Gr Forum 31(3pt2):1075–1084. https://doi.org/10.1111/j.1467-8659.2012.03100.x

Kim KI, Franz MO, Scholkopf B (2005) Iterative kernel principal component analysis for image modeling. IEEE Trans Pattern Anal Mach Intell 27(9):1351–1366. https://doi.org/10.1109/TPAMI.2005.181

Kuhn A, Lindow N, Günther T, Wiebel A, Theisel H, Hege HC (2013) Trajectory density projection for vector field visualization

Liang R, Wang Z, Zhang S, Feng Y, Jiang L, Ma X, Chen W, Tate DF (2016) Visual exploration of hardi fibers with probabilistic tracking. Inf Sci 330(C):483–494. https://doi.org/10.1016/j.ins.2015.04.045

Mallo O, Peikert R, Sigg C, Sadlo F (2005) Illuminated lines revisited. IEEE Visual 2005:19–26. https://doi.org/10.1109/VISUAL.2005.1532772

Melek Z, Mayerich D, Yuksel C, Keyser J (2006) Visualization of fibrous and thread-like data. IEEE Trans Visual Comput Gr 12(5):1165–1172. https://doi.org/10.1109/TVCG.2006.197

O'Donnell L, Kubicki M, Shenton M, Dreusicke M, Grimson W, Westin C (2006) A method for clustering white matter fiber tracts. Am J Neuroradiol 27(5):1032–1036

Park SW, Yu H, Hotz I, Kreylos O, Linsen L, Hamann B (2006) Structure-accentuating dense flow visualization. In: Proceedings of the 8th Joint Eurographics/IEEE VGTC Conference on Visualization, EUROVIS'06, pp. 163–170. Eurographics Association, Aire-la-Ville. https://doi.org/10.2312/VisSym/EuroVis06/163-170

Prasad G, Joshi SH, Jahanshad N, Villalon-Reina J, Aganj I, Lenglet C, Sapiro G, McMahon KL, de Zubicaray GI, Martin NG, Wright MJ, Toga AW, Thompson PM (2014) Automatic clustering and population analysis of white matter tracts using maximum density paths. NeuroImage 97:284–295. https://doi.org/10.1016/j.neuroimage.2014.04.033

Rinzivillo S, Pedreschi D, Nanni M, Giannotti F, Andrienko N, Andrienko G (2008) Visually driven analysis of movement data by progressive clustering. Inf Visual 7(3):225–239. https://doi.org/10.1057/palgrave.ivs.9500183

Rodriguez A, Laio A (2014) Clustering by fast search and find of density peaks. Science 344(6191):1492–1496. https://doi.org/10.1126/science.1242072

Ros C, Güllmar D, Stenzel M, Mentzel H-J, Reichenbach JR (2014) Atlas-guided cluster analysis of large tractography datasets. PLoS One 8(12):1–24. https://doi.org/10.1371/journal.pone.0083847

Sherbondy A, Akers D, Mackenzie R, Dougherty R, Wandell B (2005) Exploring connectivity of the brain's white matter with dynamic queries. IEEE Trans Visual Comput Gr 11(4):419–430. https://doi.org/10.1109/TVCG.2005.59

Tax CMW, Chamberland M, van Stralen M, Viergever MA, Whittingstall K, Fortin D, Descoteaux M, Leemans A (2015) Seeing more by showing less: orientation-dependent transparency rendering for fiber tractography visualization. PLoS One 10(10):1–20. https://doi.org/10.1371/journal.pone.0139434

Tun B, Parker WA, Ingalhalikar M, Verma R (2014) Automated tract extraction via atlas based adaptive clustering. NeuroImage 102:596–607. https://doi.org/10.1016/j.neuroimage.2014.08.021

Wei J, Yu H, Chen JH, Ma KL (Oct 2011) Parallel clustering for visualizing large scientific line data. In: 2011 IEEE Symposium on Large Data Analysis and Visualization, pp 47–55. https://doi.org/10.1109/LDAV.2011.6092316

Weri C, Song Z, Stephfan C, Ebert DS (2008) Abstractive representation and exploration of hierarchically clustered diffusion tensor fiber tracts. Comput Gr Forum 27(3):1071–1078. https://doi.org/10.1111/j.1467-8659.2008.01244.x

Zheng Y, Jeon B, Xu D, Wu QJ, Zhang H (2015) Image segmentation by generalized hierarchical fuzzy c-means algorithm. J Intell Fuzzy Syst 28(2):961–973. https://doi.org/10.3233/IFS-141378